NUCLEAR THEORY, Vol. 35 (2016)
eds. M. Gaidarov, N. Minkov, Heron Press, Sofia

Theoretical Optical Potential Derived From Chiral Potentials

M. Vorabbi[1,2], **P. Finelli**[3], **C. Giusti**[2]

[1]TRIUMF, 4004 Wesbrook Mall, Vancouver, British Columbia, V6T 2A3, Canada

[2]Dipartimento di Fisica, Università degli Studi di Pavia and INFN, Sezione di Pavia, Via A. Bassi 6, I-27100 Pavia, Italy

[3]Dipartimento di Fisica e Astronomia, Università degli Studi di Bologna and INFN, Sezione di Bologna, Via Irnerio 46, I-40126 Bologna, Italy

Abstract. Elastic scattering is probably the main event in the interactions of nucleons with nuclei. Even if this process has been extensively studied in the last years, a consistent description, i.e. starting from microscopic two- and many-body forces connected by the same symmetries and principles, is still under development. In this contribution we study the domain of applicability of microscopic two-body chiral potentials in the construction of an optical potential. We basically follow the Kerman, McManus, and Thaler approach to build a microscopic complex optical potential and then we perform some test calculations on ^{16}O at different energies. Our conclusion is that a particular set of potentials with a Lippmann-Schwinger cutoff at relatively high energies (above 500 MeV) has the best performances reproducing the scattering observables. Our work shows that building an optical potential within Chiral Perturbation Theory is a promising approach to the description of elastic proton scattering, in particular, in view of the future inclusion of many-body forces that naturally arise in such framework.

1 Introduction

A suitable and successful framework to describe the nucleon-nucleus (NA) interaction in the elastic scattering is provided by the nuclear optical potential [1]. With this instrument we can compute the scattering observables for the elastic NA scattering across wide regions of the nuclear landscape. The use of the optical potential has been also extended to calculations of inelastic scattering and other nuclear reactions, but in this work we only consider the elastic proton scattering.

The optical potential can be obtained phenomenologically [2, 3], by assuming a form of the potential and a dependence on a number of parameters adjusted to optimize the fit to the experimental data of elastic NA scattering. Alternatively and more fundamentally, it can be obtained microscopically. With suitable

approximations, microscopic optical potentials are usually derived from two basic quantities: the nucleon-nucleon (NN) t matrix and the matter distribution of the nucleus. All these models based on the NN interaction are nonrelativistic (see Ref. [4] for a detailed review). Because microscopic optical potentials do not contain adjustable parameters, we expect that they have a greater predictive power when applied to situations where experimental data are not yet available, such as, for instance, to the study of unstable nuclei.

The theoretical justification for the NA optical potential built in terms of underlying NN scattering amplitudes was given for the first time by Chew [5] and Watson *et al.* [6, 7] more than 60 years ago, and successively, by Kerman, McManus, and Thaler (KMT) [8] who developed the Watson multiple scattering approach expressing the NA optical potential by a series expansion in terms of the free NN scattering amplitudes. Several years later, with the development of high accuracy NN potentials, there has been a renewed interest in finding a rigorous treatment of the NA scattering theory in momentum space. Several authors contributed to the development of the multiple scattering theory and, with a series of papers [9–32], to calculations of microscopic optical potentials. The present work is framed in this context and it is based on the model described in Ref. [33].

The NN potential is an essential ingredient in the NA scattering theory and its off-shell properties play an important role. To obtain a good description of these properties, the optical potential models have always employed "realistic" potentials, in which the experimental NN phase shifts are reproduced with a χ^2 per data $\simeq 1$. The most commonly used NN potentials are those given by groups from Nijmegen [34], Paris [35], Bonn [36], and Argonne [37]. Successively, with the advent of the Chiral Perturbation Theory (ChPT) [38] it has been possible to calculate the NN potential perturbatively in the chiral expansion and iterate it to all orders in a Schrödinger or Lippmann-Schwinger (LS) equation to obtain the nuclear amplitude.

The most recent available chiral potentials are developed at fourth order ($\mathrm{N^3LO}$) in the chiral expansion and are used in this work as a basic ingredient to compute the NN t matrix for the construction of the NA optical potential. In particular, in all the calculations presented in this paper we adopt the two different versions of chiral potentials developed by Entem and Machleidt (EM, Refs. [39–43]), and Epelbaum, Glöckle, and Meißner (EGM, Ref. [44]).

The second important ingredient of the NA scattering theory is the microscopic structure of the nuclear target, given by neutron and proton densities. These quantities are computed within the Relativistic Mean-Field (RMF) description [45] of spherical nuclei using a Density-Dependent Meson-Exchange (DDME) model, where the couplings between mesonic and baryonic fields are assumed as functions of the density itself [46].

Our contribution is organized as follows. In Section 2 we describe the theoretical framework used to calculate the NA optical potential and we discuss the approximations made in the model. In Section 3 we present theoretical re-

sults for the scattering observables on ^{16}O calculated with all NN potentials. Predictions based on EM and EGM potentials are compared with available experimental data in order to determine the most successful theoretical approach and the best LS cutoff. In this section we also present results for the differential cross section and the analyzing power for the oxygen isotopic chain, computed with the EM potential. Finally, in Section 4 we draw our conclusions.

2 Theoretical Framework

The general problem of the elastic scattering of a proton from a target nucleus of A nucleons can be stated in momentum space by the full $(A+1)$-body Lippmann-Schwinger equation

$$T = V + VG_0(E)T\,, \tag{1}$$

whose general solution is beyond present capabilities. A reliable method to treat Eq. (1) is given by the spectator expansion [29], in which the multiple scattering theory is expanded in a finite series of terms where the target nucleons interact directly with the incident proton. In particular, the first term of this series only involves the interaction of the projectile with a single target nucleon, the second term involves the interaction of the projectile with two target nucleons, and so on to the subsequent orders. In the standard approach to elastic scattering, Eq. (1) is separated into two equations. The first one is an integral equation for T

$$T = U + UG_0(E)PT\,, \tag{2}$$

where U is the optical potential operator, and the second one is an integral equation for U

$$U = V + VG_0(E)QU\,. \tag{3}$$

The operator V represents the external interaction and the total Hamiltonian for the $(A+1)$-nucleon system is given by $H_{A+1} = H_0 + V$. If we assume the presence of only two-body forces, the operator V is expressed as $V = \sum_{i=1}^{A} v_{0i}$, where the two-body potential v_{0i} describes the interaction between the incident proton and the ith target nucleon. The system is asymptotically an eigenstate of the free Hamiltonian H_0 and $G_0(E)$ is the free propagator for the $(A+1)$-nucleon system

$$G_0(E) = \frac{1}{E - H_0 + i\epsilon}\,. \tag{4}$$

The free Hamiltonian is given by $H_0 = h_0 + H_A$, where h_0 is the kinetic energy operator of the projectile and H_A is the target Hamiltonian, $H_A\,|\Phi_A\rangle = E_A\,|\Phi_A\rangle$, where $|\Phi_A\rangle$ is the ground state of the target. The operators P and Q in Eqs. (2) and (3) are projection operators and they fulfill the condition $P+Q = \mathbb{1}$. In the case of elastic scattering P projects onto the elastic channel and can be defined as

$$P = \frac{|\Phi_A\rangle\,\langle\Phi_A|}{\langle\Phi_A|\Phi_A\rangle}\,. \tag{5}$$

With these definitions, the elastic transition operator may be defined as $T_{\rm el} = PTP$, and, in this case, Eq. (2) becomes

$$T_{\rm el} = PUP + PUPG_0(E)T_{\rm el}\,. \tag{6}$$

Thus the transition operator for elastic scattering is given by a one-body integral equation. In order to solve Eq. (6) we need to know the operator PUP. In the spectator expansion the operator U is expanded as

$$U = \sum_{i=1}^{A} \tau_i + \sum_{i,j\neq i}^{A} \tau_{ij} + \sum_{i,j\neq i,k\neq i,j}^{A} \tau_{ijk} + \cdots\,, \tag{7}$$

according to the number of nucleons interacting with the projectile. In the present work we only consider the first-order term of this expansion and, moreover, we assume the Impulse Approximation (IA) which consists in replacing the τ_i operator with the t_{0i} operator defined as

$$t_{0i} = v_{0i} + v_{0i}g_i t_{0i}\,, \qquad g_i = \frac{1}{(E - E^i) - h_0 - h_i + i\epsilon}\,. \tag{8}$$

In Eq. (8) the matrix t_{0i} represents the free NN t matrix and in the IA we only have to solve a two-body equation.

In order to develop a theoretical framework to compute the optical potential and the transition amplitude for the elastic scattering observables, we follow the path outlined in Ref. [47], that is based on the KMT multiple scattering theory and that, at the first order, is equivalent to the IA.

After some manipulations [47] the KMT first-order optical potential is obtained in the optimum factorization approximation as the product of the NN t matrix and the nuclear matter density,

$$U(\boldsymbol{q}, \boldsymbol{K}; \omega) = \frac{A-1}{A}\,\eta(\boldsymbol{q}, \boldsymbol{K}) \sum_{N=n,p} t_{pN}\left[\boldsymbol{q}, \frac{A+1}{A}\boldsymbol{K}; \omega\right]\,\rho_N(q)\,, \tag{9}$$

where $\boldsymbol{q}$ and $\boldsymbol{K}$ are the momentum transfer and the total momentum in the NA reference frame, respectively; $N = n, p$, t_{pN} represents the proton-proton (*pp*) and proton-neutron (*pn*) t matrix, ρ_N the neutron and proton profile density, and $\eta(\boldsymbol{q}, \boldsymbol{K})$ is the Møller factor, that imposes the Lorentz invariance of the flux when we pass from the NA to the NN frame in which the t matrices are evaluated. The optimally factorized optical potential given in Eq. (9) exhibits nonlocality and off-shell effects through the dependence of η and t_{pN} upon $\boldsymbol{K}$. The energy ω at which the matrices t_{pN} are evaluated is fixed at one half of the kinetic energy of the projectile in the laboratory system.

3 The Scattering Results

In this section we present and discuss our numerical results for the NA elastic scattering observables calculated with the microscopic optical potential obtained

within the theoretical framework described in the previous section. As a study case in our calculations we consider elastic proton scattering on ^{16}O.

We investigate the sensitivity of our results to the choice of the NN potential and, in particular, their dependence on the cutoff values. In order to investigate and emphasize the differences between the different NN potentials, the scattering observables have been calculated at different energies for which experimental data are available. In light of the fact that chiral potentials are based upon a low-momentum expansion, energies above 300 MeV may be considered beyond the limit of applicability of such potentials.

With these calculations we intend to achieve the following goals: 1) to check the agreement of our theoretical predictions with the empirical data; 2) to study the limits of applicability of chiral potentials in terms of the proton energy; 3) to identify the best set of values for the LS cutoffs.

In Figures 1 and 2 we show the differential cross section ($d\sigma/d\Omega$), the analyzing power A_y, and the spin rotation Q for elastic proton scattering on ^{16}O as functions of the center-of-mass scattering angle θ for two energies ($E = 100$, and 200 MeV). In the left panels we show the results obtained with the EM potentials [39–41, 43] while in the right panels we show the results obtained with the EGM potentials [44]. All potentials are denoted by the value of the LS cutoff.

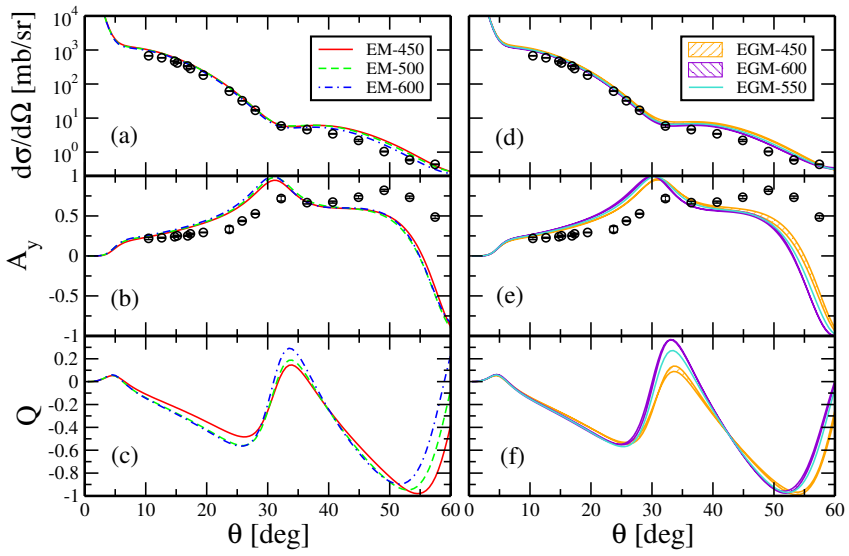

Figure 1. Scattering observables (differential cross section $d\sigma/d\Omega$, analyzing power A_y, and spin rotation Q) as a function of the center-of-mass scattering angle θ for elastic proton scattering on ^{16}O computed at 100 MeV (laboratory energy). On the left panel we employ the set of EM potentials [39–41, 43] while in the right panel we show the EGM potentials [44]. All potentials are denoted by the value of the LS cutoff. Data are taken from Refs. [48, 49].

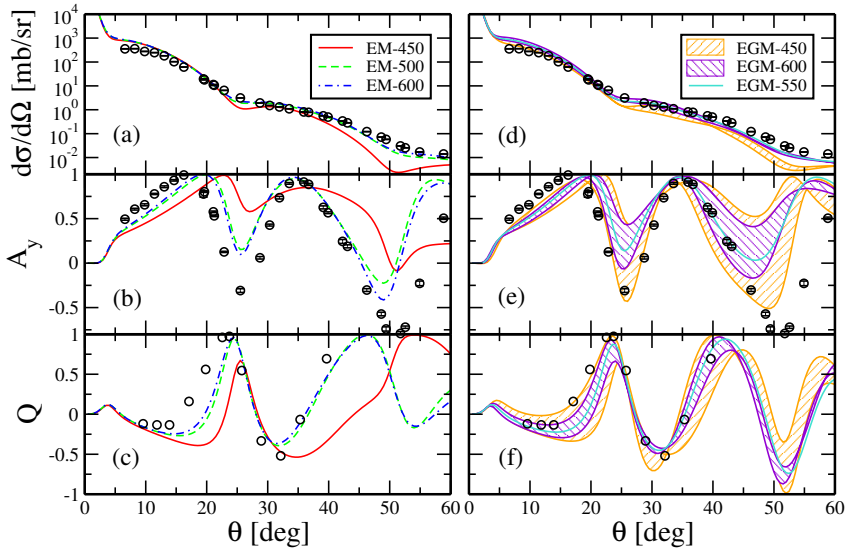

Figure 2. The same as is Figure 1 but for an energy of 200 MeV. Data are taken from Refs. [48, 49].

In Figure 1, at 100 MeV, all sets of potentials, regardless of cutoffs and theoretical approaches, give very similar results for all three observables, with the exception of A_y above 50 degrees, where all potentials overestimate the experimental data up to the maximum and then display an unrealistic downward trend, and Q around the maximum at 30 degrees. In particular, the experimental cross section is well reproduced by all potentials in the minimum region, between 30 and 35 degrees. Polarization observables are usually more sensitive to the differences in the potentials and to the ingredients and approximations of the model. Experimental data for such observables are usually more difficult to reproduce. Even if differences are rather small, potentials with the largest cutoff ($\Lambda = 600$ MeV) seem to provide the best description of A_y. The same calculations have been also performed at 135 MeV and we obtained the same results.

In Figure 2 we plot the results obtained at 200 MeV. At this energy, it is clear that potentials obtained with the lower cutoffs (EM-450 and EGM-450) cannot be employed any further: in both cases, the differential cross sections are not satisfactorily reproduced and the behaviour of A_y and Q as a function of θ is in clear disagreement with the empirical one. On the other hand, the remaining sets of potentials well describe the experimental cross sections and the analyzing power A_y, that is reasonably described not only for small scattering angles but also for values larger than the minimum value up to about 45 degrees.

On the basis of all these results for ^{16}O we can draw two conclusions: 1) Potentials with lower cutoffs cannot reproduce experimental data at energies close to 200 MeV. 2) There is no appreciable difference in using 500 or 600 MeV as

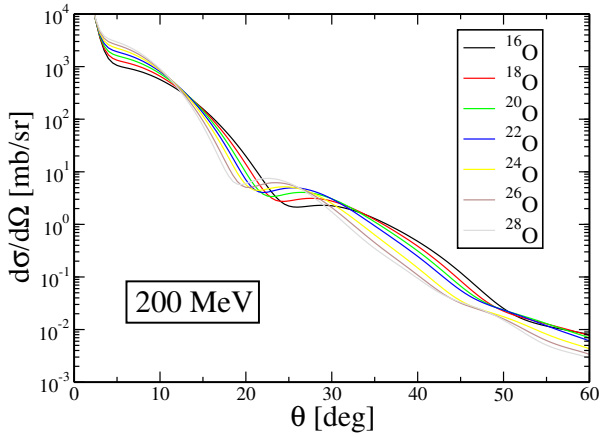

Figure 3. Theoretical results for the differential cross sections of the oxygen chain computed at 200 MeV using the EM-500 chiral potential.

LS cutoffs, even if the EM-600 and EGM-600 potentials seem to have a slightly better agreement with empirical data, in particular looking at polarization observables.

For energies above 200 MeV, this behaviour changes and the agreement with the experimental data begins to fail. This failure becomes larger as the energy increases. At energies above 300 MeV, all potentials are unable to describe the data.

Finally, in Figures 3 and 4 we display our results of the differential cross section and the analyzing power for the oxygen isotopic chain computed at 200 MeV using the EM-500 chiral potential. These results show an evolution of the scattering observables without any discontinuities along all the chain and a behavior somewhat similar to that obtained for the elastic electron scattering on the same chain [50]. In Figure 3 we observe that increasing the neutron number the magnitude of the cross section increases while its first minimum is shifted toward smaller angles, *i.e.*smaller momentum transfer. This behavior can be entirely ascribed to the nuclear densities, which generally show more pronounced differences for heavier isotopes and, consequently, produce a gradual increase of the neutron radius with increasing neutron number. The same behavior is reflected in the results for the analyzing power, displayed in Figure 4, where we observe the shift of the first minimum and the corresponding increase of its magnitude. We also note that the positions of the maxima are shifted too, but their magnitudes almost remain constant.

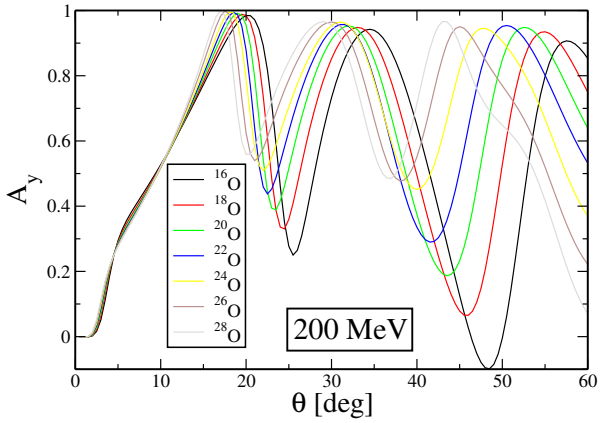

Figure 4. The same as Figure 3 but for the analyzing power.

4 Conclusions

In this work we have presented a microscopic optical potential for elastic proton-nucleus scattering. Our optical potential has been derived at the first-order term within the spectator expansion of the nonrelativistic multiple scattering theory. In the interaction between the projectile and the target nucleon, which is described by the NN τ matrix, we have neglected medium effects and we have adopted the impulse approximation, that consists in replacing τ by the free NN t matrix.

As a further simplification, we have adopted the optimum factorization approximation, where the optical potential is given in a factorized form by the product of the free NN t matrix and the nuclear density. This form conserves the off-shell nature of the optical potential and it has been used in this work to compute the cross sections and the polarization observables of elastic proton-nucleus scattering.

Two basic ingredients underlie the calculation of our microscopic optical potential: the NN interaction and a model for nuclear densities. For the NN interaction we have used two different versions of the chiral potential at fourth order ($\mathrm{N^3LO}$) based on the work of Entem and Machleidt (EM) [39–41, 43] and Epelbaum, Glöckle, and Meißner (EGM) [44], which differ in the regularization scheme employed in the two-pion exchange term and in the choice of the cutoffs. Neutron and proton densities have been computed within the RMF description [46] of spherical nuclei using a DDME model [46].

As case study for our investigation we have considered elastic proton scattering on ^{16}O. Results for the cross section, the analyzing power, and the spin rotation have been presented and discussed in comparison with available experimental data. Calculations have been performed with different NN potentials at 100 and 200 MeV.

The comparison between the results obtained with the different versions of the chiral potential represents a useful test of the reliability of our new optical potentials and allows us to identify the best set of LS cutoff values.

Polarization observables are more sensitive to the differences in the NN interactions and to the approximations of the model. This sensitivity makes it difficult to describe the experimental analyzing powers over the whole scattering angular distribution. The optical potentials obtained from all the NN potentials give close results and a good description of the experimental cross sections at 100 MeV. Of course, the differences among the results obtained with different NN potentials increase with the energy and with the scattering angle. Our results indicate that EM-600 and EGM-600 provide a slightly better agreement with empirical data for energies up to 200 MeV.

The case of elastic proton scattering considered in this work represents the first natural and necessary test of the reliability of an optical potential. The optical potential, however, represents a crucial and critical input for calculations over a wide variety of nuclear reactions and can therefore be employed in many other situations beyond those considered in this paper.

References

[1] P.E. Hodgson, *The Optical Model of Elastic Scattering*, Clarendon Press, (1963).
[2] R.L. Varner, *et al.*, *Phys. Rept.* **201** (1991) 57-119.
[3] A.J. Koning and J.P. Delaroche, *Nucl. Phys.* **A713** (2003) 231-310.
[4] J.W. Negele and E. Vogt, *Advances in Nuclear Physics* **25** (2006) 275-536.
[5] G.F. Chew, *Phys. Rev.* **80** (1950) 196-202.
[6] K.M. Watson, *Phys. Rev.* **89** (1953) 575-587.
[7] N.C. Francis and K.M. Watson, *Phys. Rev.* **92** (1953) 291-303.
[8] A.K. Kerman, H. McManus, and R.M. Thaler, *Annals of Physics* **8** (1959) 551-635.
[9] R. Crespo, R. C. Johnson, and J.A. Tostevin, *Phys. Rev. C* **41** (1990) 2257-2262.
[10] R. Crespo, R.C. Johnson, and J.A. Tostevin, *Phys. Rev. C* **46** (1992) 279-297.
[11] R. Crespo, R.C. Johnson, and J.A. Tostevin, *Phys. Rev. C* **48** (1993) 351-356.
[12] R. Crespo, R.C. Johnson, and J.A. Tostevin, *Phys. Rev. C* **50** (1994) 2995-3009.
[13] H.F. Arellano, F.A. Brieva, and W.G. Love, *Phys. Rev. Lett.* **63** (1989) 605-608.
[14] H.F. Arellano, F.A. Brieva, and W.G. Love, *Phys. Rev. C* **41** (1990) 2188-2201.
[15] H.F. Arellano, F.A. Brieva, and W.G. Love, *Phys. Rev. C* **42** (1990) 652-658.
[16] H.F. Arellano, *et al.*, *Phys. Rev. C* **43** (1991) 1875-1880.
[17] H.F. Arellano, F.A. Brieva, and W.G. Love, *Phys. Rev. C* **50** (1994) 2480-2489.
[18] H.F. Arellano, F.A. Brieva, and W.G. Love, *Phys. Rev. C* **52** (1995) 301-315.
[19] H.F. Arellano, *et al.*, *Phys. Rev. C* **54** (1996) 2570-2581.
[20] H.F. Arellano and E. Bauge, *Phys. Rev. C* **76** (2007) 014613.
[21] F.J. Aguayo and H.F. Arellano, *Phys. Rev. C* **78** (2008) 014608.
[22] H.F. Arellano and E. Bauge, *Phys. Rev. C* **84** (2011) 034606.
[23] Ch. Elster and P.C. Tandy, *Phys. Rev. C* **40** (1989) 881-886.
[24] Ch. Elster, *et al.*, *Phys. Rev. C* **41** (1990) 814-827.

[25] C.R. Chinn, Ch. Elster, and R.M. Thaler, *Phys. Rev. C* **44** (1991) 1569-1580.
[26] Ch. Elster, L.C. Liu, and R.M. Thaler, *Journal of Physics G: Nuclear and Particle Physics* **19** (1993) 2123-2134.
[27] C.R. Chinn, Ch. Elster, and R.M. Thaler, *Phys. Rev. C* **47** (1993) 2242-2249.
[28] C.R. Chinn, Ch. Elster, and R.M. Thaler, *Phys. Rev. C* **48** (1993) 2956-2966.
[29] C.R. Chinn, *et al.*, *Phys. Rev. C* **52** (1995) 1992-2003.
[30] Ch. Elster, S.P. Weppner, and C.R. Chinn, *Phys. Rev. C* **56** (1997) 2080-2092.
[31] S.P. Weppner, Ch. Elster, and D. Hüber, *Phys. Rev. C* **57** (1998) 1378-1385.
[32] Ch. Elster, A. Orazbayev, and S.P. Weppner, *Few-Body Systems* **54** (2013) 1399-1403.
[33] M. Vorabbi, P. Finelli, and C. Giusti, *Phys. Rev. C* **93** (2016) 034619.
[34] V.G.J. Stoks, *et al.*, *Phys. Rev. C* **49** (1994) 2950-2962.
[35] M. Lacombe, *et al.*, *Phys. Rev. C* **21** (1980) 861-873.
[36] R. Machleidt, *Advances in Nuclear Physics* **19** (1989) 189-376.
[37] R.B. Wiringa, V.G.J. Stoks, and R. Schiavilla, *Phys. Rev. C* **51** (1995) 38-51.
[38] S. Scherer, *Adv. Nucl. Phys.* **27** (2003) 277.
[39] D.R. Entem and R. Machleidt, *Phys. Rev. C* **68** (2003) 041001.
[40] E. Marji, *et al.*, *Phys. Rev. C* **88** (2013) 054002.
[41] L. Coraggio, *et al.*, *Phys. Rev. C* **87** (2013) 014322.
[42] F. Sammarruca, *et al.*, *Phys. Rev. C* **91** (2015) 054311.
[43] L. Coraggio, *et al.*, *Phys. Rev. C* **75** (2007) 024311.
[44] E. Epelbaum, W. Glöckle, and Ulf-G. Meißner, *Nucl. Phys. A* **747** (2005) 362-424.
[45] T. Nikšić, *et al.*, *Computer Physics Communications* **185** (2014) 1808-1821.
[46] T. Nikšić, *et al.*, *Phys. Rev. C* **66** (2002) 024306.
[47] A. Picklesimer, *et al.*, *Phys. Rev. C* **30** (1984) 1861-1879.
[48] http://www.physics.umd.edu/enp/jjkelly/datatables.htm.
[49] http://www.nndc.bnl.gov/exfor/exfor.htm.
[50] A. Meucci, *et al.*, *Phys. Rev. C* **87** (2013) 054620.